Structural and Kinetic Determinants of Aldehyde Reduction by Aldose Reductase†

Sanjay Srivastava,‡ Stanley J. Watowich,‡ J. Mark Petrash,§ Satish K. Srivastava,*,‡ and Aruni Bhatnagar‡,||

Department of Human Biological Chemistry and Genetics, 619 Basic Science Building, and Physiology and Biophysics, University of Texas Medical Branch, Galveston, Texas 77555, and Department of Ophthalmology and Visual Sciences and of Genetics, Washington University, St. Louis, Missouri 63110

Received July 24, 1998; Revised Manuscript Received September 25, 1998

ABSTRACT: Aldose reductase (AR) is a member of the aldo-keto reductase superfamily. Due to its ability to catalyze the formation of sorbitol from glucose during hyperglycemic and hypertonic stress, the aldose-reducing property of AR has been accepted as its main physiological and pathological function. Nonetheless, AR is a poor catalyst for glucose reduction and displays active-site properties unexpected of a carbohydrate-binding protein. We, therefore, examined the catalytic properties of AR with a series of naturally occurring aldehydes, compatible in their hydrophobicity to the large apolar active site of the enzyme. Our results show that recombinant human AR is an efficient catalyst for the reduction of medium- to long-chain unbranched saturated and unsaturated aldehydes. The enzyme displayed selective preference for saturated aldehydes, such as hexanal, and unsaturated aldehydes, such as *trans*-2-octenal and nonenal as well as their 4-hydroxy derivatives. Short-chain aldehydes such as propanal and acrolein were reduced less efficiently. Branched derivatives of acrolein or its glutathione conjugate (GS-propanal) were, however, reduced with high efficiency. In the absence of NADPH, the α, β unsaturated aldehydes caused covalent modification of the enzyme. On the basis of electrospray mass spectrometric analysis of the wild-type and site-directed mutants of AR (in which the solvent exposed cysteines were individually replaced with serine), the site of modification was identified to be the active-site residue, Cys 298. The unsaturated aldehydes, however, did not modify the enzyme bound to NADPH and did not inactivate the enzyme during catalysis. Modeling studies indicate that the large hydrophobic active site of AR can accommodate a large number of aldehydes without changes in the structure of the binding site or movement of side chains. High hydrophobicity due to long alkyl chains or apolar substituents appears to stabilize the interaction of the aldehyde substrates with the enzyme. Apparently, such hydrophobic interactions provide substrate selectivity and catalytic efficiency of the order achievable by hydrogen bonding. Since several of the aldehydes reduced by AR are either environmental and pharmacological pollutants or products of lipid peroxidation, the present studies provide the basis of future investigations on the role of AR in regulating aldehyde metabolism particularly under pathological states associated with oxidative stress and/or aldehyde toxicity.

INTRODUCTION

Aldose reductase (AR) is a member of the aldo-keto reductase superfamily of enzymes (*1*). It represents the first step of the polyol pathway and catalyzes the reduction of glucose to sorbitol. Since high concentrations of polyols accumulate during sugar cataracts, and pharmacological inhibition of AR prevents, delays, or, in some cases, even reverses tissue injury associated with several secondary diabetic complications, it has been suggested that increased flux of glucose via the AR-catalyzed pathway is a significant cause of hyperglycemic injury (*1, 2*). These data, obtained with diabetic humans and animals, have been taken as prima facie evidence supporting a primary role of AR in glucose metabolism (hence the name "aldose" reductase). Nevertheless, the physiological role of AR is unlikely to be restricted to hyperglycemic metabolism. The enzyme is widely distributed in organisms ranging from yeast to man and is expressed in particularly high levels in several insulin-dependent tissues, e.g., heart and skeletal muscle (*1, 3*−*6*) in which the cellular concentrations of glucose do not attain high levels. Furthermore, the structural, thermodynamic, and kinetic features of AR are not well suited for catalysis of sugar metabolism. The active site of the enzyme lacks polar residues, which through hydrogen bonds provide high specificity and affinity to all other carbohydrate-binding proteins (*7*). In fact, in vitro AR displays poor affinity for glucose with a $K_m \approx 50-100$ mM (*1*), indicating that at least under euglycemic conditions, glucose metabolism may not be the primary physiological function of this enzyme.

Studies with the purified AR show that it is an efficient catalyst for the reduction of a wide range of aldehydes (*1, 8*). In particular, the enzyme displays high affinity for hydrophobic aldehydes, e.g., 4-hydroxy *trans*-2-nonenal (HNE), which are generated during peroxidation of membrane lipids (*9, 10*). Due to their high electrophilicity,

† This work was supported in part by NIH Grants HL55477, HL59378, DK20579, and DK36118.

* To whom correspondence should be addressed. Tel: (409) 772-3926. Fax: (409) 772-9679. E-mail: ssrivast@utmb.edu.

‡ Department of Human Biological Chemistry and Genetics.

§ Washington University.

|| Physiology and Biophysics.

10.1021/bi981794l CCC: $18.00
Published on Web 12/10/1998

unsaturated aldehydes such as HNE are particularly damaging to cellular metabolism and could extend, mediate, and amplify the cellular effects of unquenched reactive oxygen species (*11*). Indeed, protein adducts of lipid-derived aldehydes have been found to accumulate under several disease states such as atherosclerosis (*11, 12*), Alzheimer (*13*), and Parkinson's disease (*14*). In addition, exocyclic adducts of aldehydes with DNA have been identified not only in animals exposed to carcinogens but also in animals and humans not exposed to carcinogens, suggesting the possibility that such adducts may represent common background lesions related to spontaneous carcinogenesis and aging (*15*).

While adducts of lipid-derived aldehydes with proteins and DNA have been widely used as markers of oxidative injury, recent evidence suggests that aldehydes derived from lipid peroxidation may indeed participate in the progression of several pathological conditions. For instance, the proliferative and cytotoxic effects of oxidized low-density lipoprotein (ox LDL) may be in part due to HNE and related aldehydes (*16, 17*). Moreover, HNE induces membrane protein dysfunction similar to that caused by the amyloid β-peptide (*18*). Thus, HNE metabolism may be an important determinant of tissue pathology associated with enhanced lipid peroxidation. Because it catalyzes the reduction of HNE, AR may represent an important route of aldehyde detoxification. However, in addition to HNE and related 4-hydroxyalkenals, lipid peroxidation also generates high concentrations of other saturated and unsaturated aldehydes such as acrolein, malonaldehyde, C4 to C9 alkanals and alkenals, and 2,4, alkadienals (*11, 19, 20*). These aldehydes display different metabolic effects (*11*) and their protein adducts elicit distinct immunological responses (*21*). The general role of AR in the metabolism of lipid-derived aldehydes as a class, however, awaits further clarification.

The present study was designed to examine whether AR catalysis is limited to HNE or if it extends to the entire range of long- and short-chain, saturated and unsaturated aldehydes generated during lipid peroxidation. To identify structural features of the substrates as well as the enzyme, which optimize catalysis, we systematically examined several classes of lipid-derived aldehydes as potential substrates of AR. In addition, we also investigated the nature of adduct between these aldehydes and AR, and the chemical mechanism by which they regulate AR activity.

MATERIALS AND METHODS

NADPH, DL-glyceraldehyde, and D,L-dithiothreitol (DTT) were purchased from Sigma Chemical Co., St. Louis, MO. Sephadex G-25 column (PD-10) was purchased from Pharmacia Fine Chemicals, Upasala, Sweden. Saturated aliphatic aldehydes, acrolein, crotonaldehyde, trans-2-alkenals, and trans,trans-2,4-alkadienals were obtained from Aldrich. The 4-hydroxy *trans*-2-pentenal, 4-hydroxy *trans*-2-hexenal, 4-hydroxy *trans*-2-octenal, and 4-hydroxy *trans*-2-decenal were generous gifts from Prof. B. Mannervik, University of Stockholm, Sweden. All the other reagents were of the highest purity available. The HNE was synthesized as its dimethyl acetal from the dimethyl acetal of fumaraldehyde as described previously (*22*). Free HNE was prepared by the acid hydrolysis (pH 3.0) of the dimethyl acetal for 1 h at room temperature. The sodium salt of malonaldehyde (MDA) was prepared by the method of Marnett and Tuttle (*23*) and its purity was determined by NMR. The recombinant human placental AR and site-directed mutant forms of the enzyme were prepared as described before (*24*).

Reduction of the Recombinant Enzyme. Before each experiment, stored AR was reduced by incubating with 0.1 M DTT at 37 °C for 1 h in 0.1 M potassium phosphate (pH 7.0). Excess DTT was removed by gel-filtration through a Sephadex G-25 column (PD-10), preequilibrated with nitrogen-saturated 0.1 M potassium phosphate, pH 7.0, containing 1 mM EDTA. All operations were carried out at 4 °C to prevent oxidation of the enzyme. The reduced enzyme was stored under nitrogen and was used within 1 h.

Measurement of Enzyme Activity. The activity of the enzyme was determined at 25 °C in a 1 mL system containing 0.1 M potassium phosphate, pH 7.0, 10 mM D,L-glyceraldehyde, and 0.1 mM NADPH. The reaction was monitored by measuring the rate of disappearance of NADPH at 340 nm using a Gilford Response^{II} spectrophotometer. One unit of enzyme activity is defined as the amount of the enzyme required to oxidize 1 μmol of NADPH/min. The control cuvette (blank) contained all components of the reaction mixture except the enzyme. The aldehyde substrates were varied over a concentration range extending from 0.2 to 5−7 times the K_m of each aldehyde. Initial velocity was measured at 6−8 different concentrations of each substrate.

Formation of Enal Conjugates. To synthesize glutathione conjugates, 75 μM each of trans-2 alkenals, 4-hydroxy trans-2-alkenals, and trans,trans-2,4-alkadienals was incubated individually with an equimolar concentration of GSH in 0.1 M potassium phosphate, pH 7.0, at room temperature. For generating lysine adducts, similar conditions were used, except that glutathione was replaced by lysine. The progress of the reactions was monitored by following the decrease in OD_{210} nm for acrolein, OD_{224} nm for other trans-2-alkenals and 4-hydroxy trans-2-alkenals, and OD_{280} nm for trans,trans-2,4-alkadienals. Conjugates of acrolein with *N*-acetylcysteine, Gly-Cys, and GSH were prepared under similar conditions and were purified by HPLC prior to use.

Molecular Modeling Studies. Modeling studies were performed with the program O (*25*). The AR structure was based on the 1.78 Å resolution structure of human AR complexed with $NADP^+$ and glucose 6-phosphate, obtained as entry 2ACQ from the Brookhaven Protein Data Bank. Crystallographic waters were removed from the crystallographic coordinate file prior to modeling studies. Coordinates for aldehyde substrates were generated with ChemDraw Plus (*26*). Aldehyde substrates were positioned manually in the enzyme active site using the program O.

Enal Modification of Aldose Reductase. Reduced AR (0.5 mg/mL) was incubated with 100 μM freshly prepared enal in 0.1 M potassium phosphate, pH 7.0, at room temperature, and aliquots of the reaction mixture were withdrawn at indicated time intervals to measure the enzyme activity as described above.

Statistical Analysis. Individual saturation curves used to obtain the steady-state kinetic parameters were fitted to a general Michaelis−Menten equation according to Cleland (*27*). In all cases, the best fit to the data was chosen on the basis of the standard error of the fitted parameters and the lowest value of σ, which is defined as the sum of squares of the residuals divided by the degrees of freedom ($n - 1$).

For steady-state kinetic analysis, *n* represents the number of velocity measurements, and in inactivation analysis, *n* is the number of time points at which the enzyme activity was measured.

The rate constants for modification of the enzyme were calculated using specific rate equations listed in the legends to the appropriate tables. In each case, the best fits of the equation to the data were chosen on the basis of the χ^2 and R^2 values calculated by nonlinear regression using NFIT (Island Products, Galveston, TX). Data are presented as ± standard error of the mean (SEM).

Electrospray Ionization-Mass Spectrometry (ESI-MS). The electrospray ionization mass spectra were obtained on a Finnigan-TSQ70 (upgraded to TSQ700) triple quadropole instrument with a Vestec electrospray ionization source with a tapered fused silica capillary needle (50 μm i.d.). Additives to the enzyme sample (DTT, acrolein, crotonaldehyde, or HNE) were removed prior to electrospray by gel filtration through a PD-10 column. The enzyme samples were electrosprayed from solution of a 1:1 mixture of the protein in 10 mM ammonium acetate and methanol/acetic acid mixture 100/10 (vol/vol). The samples were at approximately 50 μg/mL. The analyte solutions were infused into the mass spectrometer source using a Harvard syringe pump at a rate of 0.82 μL/min. The spray voltage was set at 3.5 kV and the nozzle voltage at 250 V, with a repeller voltage of 9−11 V. A source temperature of 229−252 °C was used. Source bath nitrogen was turned off or set to 1.8 or 3.2 psi as needed to achieve good spectra for standard proteins and left at the same setting for the samples analyzed on that day. The Quad 3 was scanned from 600 to 200 amu/3 s, and 128 scans were averaged before data were acquired to a file. Spectra were deconvoluted using an input mass range (InMR) of 600−200 Da, an output mass range of 10 000−40 000 Da, mass step of 0.1, and a peak width of 2 amu, using a deconvolution algorithm (BioMass, FinniganMAT). In all cases, the standard errors in mass determinations ranged between 1.5 and 2.5 mass units, which were similar to the errors calculated with the protein standard (apomyoglobin and bovine serum albumin) used to calibrate the instrument.

RESULTS

Steady-State Kinetics. The unsaturated aldehydes tested in this study are highly reactive and readily form covalent adducts with proteins (*11*). Because AR contains reactive thiols as well as lysine residues, it is possible that their modification by electrophilic aldehydes may confound steady-state measurements. To test this, we studied the progression curves of AR with HNE as the substrate. In these experiments, oxidation of NADPH by HNE was monitored as a function of time at different concentrations of the enzyme. Since

$$[E]_0 t = f(y, k, [X]_0)$$

where k represents the rate constant of the reaction, $[X]_0$ is the initial substrate concentration, and $[E]_0$ is the total enzyme concentration, plots of y (product formed) versus $[E]_0 t$ (Selwyn's plot) obtained at several enzyme concentrations are superimposable unless the enzyme, the substrates, or the products are unstable (*28*). As shown in Figure 1, the plots of NADP generated versus $[AR]_0 t$ were virtually superimposable, and the scatter in the data points is well within the error range of these measurements, indicating that AR does not undergo progressive inactivation in the assay, and that there are no significant uncatalyzed side reactions between HNE and NADPH or HNE and the assay mixture. On the basis of these data, we conclude that during catalysis there is no significant inactivation of AR by HNE, and thus simple steady-state analyses could be used to estimate the kinetic parameters of the enzyme with these aldehydes.

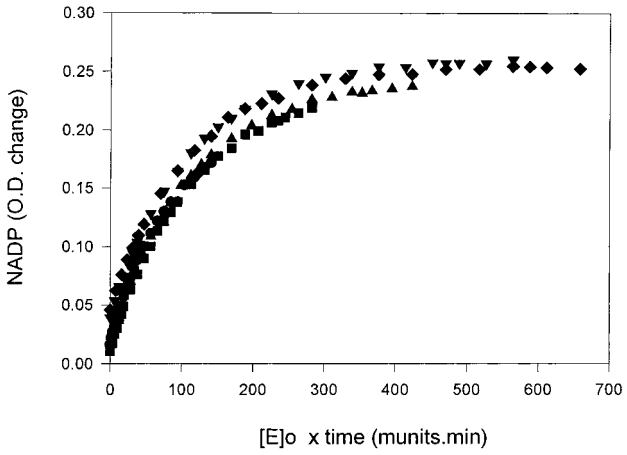

FIGURE 1: Selwyn's plot for aldose reductase-catalyzed reduction of HNE. Time-dependent changes in NADP formation (estimated from an increase in A_{340}) are plotted at the indicated enzyme concentrations (in milliunits) × time.

The kinetic parameters for AR-catalyzed reduction of saturated and unsaturated aldehydes are summarized in Table 1. Under the experimental conditions used, all the aldehydes tested displayed Michaelis−Menten kinetics. For saturated aldehydes (alkanals), the K_m values for the long-chain aldehydes were generally lower than that for the short-chain compounds. While the enzyme displayed a relatively high K_m for propanal (~5 mM), the K_m decreased by 2 orders of magnitude for butanal, which contains only an additional methylene group. The decrease in K_m with increase in the carbon chain length from 4 to 6 was accompanied by a corresponding increase in the catalytic efficiency (k_{cat}/K_m). For alkanals with more than six carbons, no further decrease in K_m was observed and the k_{cat}/K_m values tended to decrease after a maxima with hexanal. Interestingly, malonaldehyde (MDA), which is generated in appreciable quantities during peroxidation of membrane lipids, was not a substrate for AR.

As with the alkanal series, the K_m values of the alkenals decreased with an increase in the carbon chain length. The only exception was acrolein, which had a 4-fold lower K_m than crotonaldehyde. However, all alkenals with carbon chain lengths longer than corotonaldehyde displayed a progressive decrease in K_m, until a chain length of eight carbons, after which no further decrease in K_m was observed. Essentially similar behavior was observed with the 4-hydroxy trans-2-alkenals, which at shorter carbon chain lengths exhibited higher K_m values than the corresponding alkanal. A comparison of straight chain trans-2-alkenals with hydroxyalkenals did not reveal additional catalytic advantage due to the presence of a hydroxyl group at C_4.

The presence of an additional double bond between C_4 and C_5 of the hydrocarbon chain had no significant effect on K_m values for hexenal. However, for C7 to C10 alkadi-

Table 1: Steady-State Kinetic Parameters for Aldose Reductase-Catalyzed Reduction of Saturated and Unsaturated Aldehydes[a]

substrate	K_m (mM)	k_{cat} (min^{-1})	k_{cat}/K_m (min^{-1} mM^{-1})
saturated aldehydes			
propanal	4.89 ± 0.410	27.0	5.5
butanal	0.0578 ± 0.005	25.4	439
pentanal	0.0108 ± 0.001	27.5	2546
hexanal	0.0070 ± 0.001	25.6	3657
heptanal	0.0076 ± 0.009	18.8	2474
ocatanal	0.0130 ± 0.001	18.8	1446
nonanal	0.0260 ± 0.004	30.1	1157
decanal	0.0160 ± 0.002	19.6	1225
unsaturated aldehydes			
acrolein	0.802 ± 0.21	37.6	47.0
crotonaldehyde	3.480 ± 0.38	35.6	10.2
trans-2-pentenal	0.419 ± 0.1	25.8	61.7
trans-2-hexenal	0.133 ± 0.023	29.5	221
trans-2-heptenal	0.098 ± 0.024	25.2	257
trans-2-octenal	0.016 ± 0.002	33.9	2119
trans-2-nonenal	0.019 ± 0.0064	39.1	2058
4-hydroxy *trans*-2-pentenal	0.136 ± 0.048	27.0	199
4-hydroxy *trans*-2-hexenal	0.168 ± 0.024	32.5	193
4-hydroxy *trans*-2-octenal	0.022 ± 0.006	13.8	628
4-hydroxy *trans*-2-nonenal	0.028 ± 0.009	25.8	921
4-hydroxy *trans*-2-decanal	0.021 ± 0.007	12.6	600
trans,trans-2,4-hexadienal	0.143 ± 0.04	19.8	139
trans,trans-2,4-heptadienal	0.087 ± 0.026	16.8	193
trans,trans-2,4-nonadienal	0.061 ± 0.009	34.3	561
trans,trans-2,4-decadienal	0.060 ± 0.01	27.9	465
trans-4-decenal	0.022 ± 0.002	24.4	1108
cis-4-decenal	0.029 ± 0.003	24.8	862
trans-2, *cis*-6-decadienal	0.010 ± 0.001	16.6	1660

[a] The enzyme activity was determined in 0.1 M potassium phosphate (pH 7.0) using the indicated aldehyde and 0.1 mM NADPH at 25 °C. The recombinant enzyme was reduced by DTT prior to measurement.

enals, the K_m values were 3-fold higher as compared to the corresponding trans-2-alkenal. No discrimination between cis and trans forms was evident [$K_{m(trans-4-decanal)} \approx K_{m(cis-4-decanal)}$]. Surprisingly, *trans*-2,*cis*-6 decandienal was a good substrate and displayed K_m values much lower than *trans,trans*-2,4-decadienal.

Since acrolein presented an anomalous case, steady-state kinetic parameters were determined with other acrolein derivatives. As shown in Table 2, derivatives with bulkier substituents at the terminal carbon displayed lower K_m values as compared to unsubstituted acrolein. Moreover, the K_m value of 2-methylacrolein was 10-fold lower than crotonaldehyde and 2-ethyl and 2-butyl acrolein exhibited 3- and 2-fold lower K_m values as compared to *trans*-2-pentenal and *trans*-2-hexenal. Similar to the behavior observed with aliphatic derivatives, the presence of a benzene ring at the third carbon of acrolein significantly decreased the K_m value, and the $K_{m(phenylacrolein)}$ and $K_{m(\alpha-methylphenylacrolein)}$, respectively, were 20- and 60-fold lower than $K_{m(acrolein)}$. Furthermore, the Michael adducts of acrolein with *N*-acetyl cysteine, cysteinylglycine, and glutathione displayed remarkably lower K_m values as compared to the parent acrolein, and their k_{cat}/K_m values were 200−800-fold higher than propanal.

Molecular Modeling Studies. A crystal structure of AR with the substrate bound to the active site is not available. Thus, modeling studies were used to investigate the potential interactions of aldehydes with AR. The AR structure was based on the 1.78 Å resolution structure of human AR complexed with $NADP^+$ and glucose 6-phosphate (*29*). This structure is similar to the structure of the AR:NADPH complex determined to 1.65 Å resolution (*7*). Only minor differences in the positions of Ser 127 and Pro 222 were noted between these two structures in the vicinity of the active site. In our modeling studies, these residues do not contact substrates bound at the active site of the enzyme.

Table 2: Steady-State Kinetic Parameters for Aldose Reductase-Catalyzed Reduction of Acrolein and Its Derivatives[a]

substrate	K_m (mM)	k_{cat} (min^{-1})	k_{cat}/K_m (min^{-1} mM^{-1})
acrolein	0.80 ± 0.21	37.6	47
2-methyl acrolein	0.33 ± 0.04	33.1	100
2-ethyl acrolein	0.13 ± 0.01	29.4	226
2-butyl acrolein	0.077 ± 0.01	26.1	339
aromatic derivatives			
phenyl acrolein	0.039 ± 0.005	23.9	613
methyl phenyl acrolein	0.013 ± 0.001	23.8	1831
conjugates			
N-acetylcysteine propanal	0.0249 ± 0.0013	42.4	1703
Gly-Cys-propanal	0.0186 ± 0.0012	29.8	1602
GS-propanal	0.0066 ± 0.0001	36.3	5500

[a] The enzyme activity was determined in 0.1 M potassium phosphate (pH 7.0) using the indicated aldehyde and 0.1 mM NADPH at 25 °C. The recombinant enzyme was reduced by DTT prior to measurement. *N*-Acetyl cysteinyl propanal, Gly-Cys-propanal, and GS-propanal were prepared by incubating stoichiometric amounts of acrolein with the thiol, as described under Materials and Methods.

Two different orientations for the aldehyde moiety of the bound substrate were examined. In case 1 (Figure 2, panels A and C), aldehyde substrates were positioned in the AR active site such that they approximated the orientation observed in the cocrystal structures of AR:glucose 6-phosphate (*29*) and AR:zopolrestat (*30*). The carbonyl carbon (C_1 atom) of the aldehyde was positioned as observed for the carbonyl carbon of bound glucose 6-phosphate and the carboxylate of zopolrestat. The aldehyde functional group is parallel to the nicotinamide ring of $NADP^+$ and the carbonyl oxygen is directed toward the amide group of the nicotinamide ring. The carbonyl oxygen of the aldehyde was positioned as observed for the carboxylate oxygen O3 of zopolrestat. The C_2 and C_3 atoms of the aldehyde were positioned as observed for the C_{17} and C_4 atoms of zopolrestat, respectively. In case 2 (Figure 2, panels B and D), aldehyde substrates were positioned in the AR active site such that they approximated the orientation determined from modeling calculations of De Winter and von Itzstein (*31*). In this orientation, the carbonyl oxygen of the aldehyde occupies the same position as in the previous (case 1) orientation. However, the alkyl chain of the substrate is flipped approximately 180° about an axis parallel to the length of the alkyl chain, thus directing the hydrogen atom of the aldehyde functional group toward the amide group of the nicotinamide ring.

Table 3 lists distances between AR and the substrates hexanal, α-methyl phenylacrolein, and 4-hydroxy *trans*-2-hexenal for each of the case 1 and case 2 orientations. In both case 1 and case 2 orientations, the carbonyl oxygen of the aldehyde is 2.6 Å from the Nϵ atom of His 110 and 3.0 Å from the hydroxy of Tyr 48 (Table 3), the carbonyl carbon C_1 atom of the aldehyde is approximately 3.1 Å from the Nϵ2 atom of His 110 (Table 3). The C_2 methylene group is

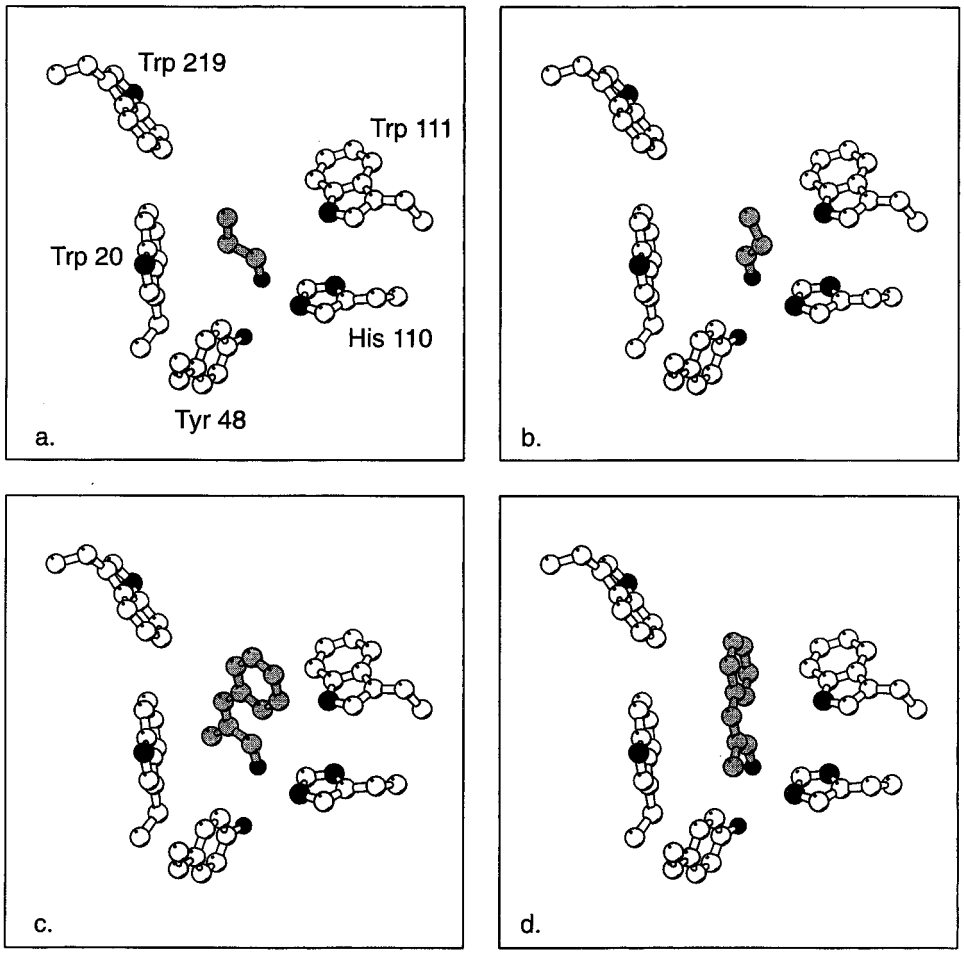

FIGURE 2: Schematic diagram (generated with Molscript) of aldehyde substrates bound at the active site of aldose reductase. All views are looking onto the plane of the nicotinamide ring of NADPH, located below the aldehyde substrate. Carbon atoms of the substrate and enzyme are shaded gray and white, respectively. Nitrogen and oxygen atoms are colored dark gray and black, respectively. (a, b) Two possible orientations for binding acrolein in the AR active site. In panel a, the aldehyde orientation approximates that observed in the AR:glucose 6-phosphate (*29*) and AR:zopolrestat (*30*) complexes, while in panel b, the binding orientation approximates that proposed by De Winter and von Itzstein (*31*). (c, d) Two possible orientations for binding 2-methyl phenylacrolein in the AR active site. The aldehydes in panels c and d are bound in the same orientations as the aldehydes in panels a and b, respectively.

within approximately 3 Å of His 110 in the case 2 orientation. No contacts are observed for the C_3 methylene group of the substrate. Hydrophobic contacts between the substrate and AR are observed for the C_4 methylene group of the alkyl chain. Subsequent methylene groups of longer alkyl substrates participate in additional hydrophobic contacts with AR.

In both case 1 and case 2 orientations, a predominantly anti conformation was modeled for the saturated alkyl chain in the active site. In this conformation, the alkanal and alkenal alkyl chains project out of the AR active site. As noted in previous crystallographic studies, the AR active site is large and highly hydrophobic, lined with residues Trp 20, Val 47, Tyr 48, Trp 79, Trp 111, Phe 121, Phe 122, Pro 218, Trp 219, Leu 300, and Leu 301. The large size of the AR active site allows the aldehyde's aliphatic chain considerable freedom to occupy several approximately equivalent positions within the AR active site and still contact the hydrophobic residues that line the active site. For example, several different extended chain conformations of the alkyl chain of nonanal can be positioned in the AR active site (Figure 3). One C_2-C_3 gauche conformation of nonanal, within an otherwise all anti conformation, results in the C_6 methylene group in contact with Val 47, the C_7 methylene group in contact with Phe 122, the C_8 and methylene group in contact Val 47 and the C_9 methylene group in contact with Phe 122. A stereochemical energy equivalent C_4-C_5 gauche conformation of nonanal results in the C_4 and C_5 methylene groups in contact with Trp 20 and Trp 219, the C_6 methylene group in contact with Trp 219, and the C_8 and C_9 methylene groups in contact with Leu 300 (Figure 3).

The hydroxyl group of 4-hydroxy trans-2-alkenal substrates can be positioned within 3.3 Å of CZ3 Trp 219 in a case 1 orientation and within 2.9 Å of CH2 Trp 79 in a case 2 orientation. Neither orientation appears to result in the formation of hydrogen bonds. Derivatives of acrolein can be positioned within the AR active site in both case 1 and case 2 orientations without steric overlaps with AR residues. These binding orientations can be accommodated without changes in the AR structure or movement of the AR side chains. The methyl group of 2-methyl acrolein and the phenyl moiety of α-methyl phenyl acrolein make extensive hydrophobic contacts with AR residues in both case 1 and case 2 orientations (Table 3).

Modification of AR by Enals. While no inactivation of the enzyme was observed during catalytic reduction of the unsaturated aldehydes (vide supra), incubation of the apoenzyme with the unsaturated aldehydes led to time- and

Table 3: Interactions between Aldose Reductase and Aldehyde Substrates Positioned in the Active Site of Aldose Reductase[a]

interaction		hexanal		α-methyl phenyl acrolein		4-hydroxy *trans* 2-hexenal	
aldehyde	aldose reductase	case 1	case 2	case 1	case 2	case 1	case 2
carbonyl oxygen	NE His 110	2.6	2.6	2.6	2.6	2.6	2.6
	CE1 His 110	3.3	3.3	3.3	3.3	3.3	3.3
	OH Tyr 48	3.0	3.0	3.0	3.0	3.0	3.0
	O7N NADPH	3.1	3.1	3.1	3.1	3.1	3.1
	C7N NADPH	3.2	3.2	3.2	3.2	3.2	3.2
carbonyl carbon (C1)	NE2 His 110	3.1	3.1	3.1	3.0	2.9	3.0
C2	NE2 His 110		2.9				2.8
	CE1 His 110		3.2				3.1
	NE1 Trp 111						3.3
C3	NE1 Trp 111						3.3
C4	CH2 Trp 20	3.2				3.3	
	CZ2 Trp 20	2.8				2.9	
	CH2 Trp 219					3.3	
	CH2 Trp 79		3.1				2.9
	CZ3 Trp 79						3.2
	NE1 Trp 111		3.2				3.0
C5	CH2 Trp 219	3.0					
	CZ3 Trp 219	3.0					
	CZ Phe 122		3.2				
	CD2 Leu 300						3.3
	NE1 Trp 111						2.8
	C5 Trp 111						3.2
	CH2 Trp 20					3.0	
C6	CH2 Trp 219	3.2					
	CD2 Leu 300						3.1
4-hydroxyl	CZ Phe 122						3.3
	CH2 Trp79						2.9
	CZ3 Trp 219					3.3	
CR2	NE1 Trp 111			3.2			
CR3	CZ3 Trp 79			3.1			
	CH2 Trp 79			2.9			
	NE1 Trp 111			2.8			
	CB Cys 298				2.9		
	SG Cys 298				2.9		
CR4	CH2 Trp 79			3.1			
	CZ Phe 122			3.2			
	CB Cys 298				3.0		
	SG Cys 298				3.3		
α-methyl	CZ3 Trp 20			3.0			
	CD2 Trp 20			3.1			
	CE1 Trp 20			2.7			
	CG1 Val 47				2.8		
	CE1 Tyr 48				2.9		
	CE1 His 110				3.1		

[a] Atom naming convention follows the Protein Data Bank. Carbon atoms CR2, CR3 and CR4 refer to the ortho, meta, and para positions of the phenyl group, respectively.

concentration-dependent modification of the enzyme. When the enzyme was incubated with short-chain aldehydes such as acrolein and crotonaldehyde, modification led to an increase in enzyme activity. The increase in activity of the enzyme was well described by single exponential. With acrolein, limiting value of 7.26 was estimated for the pre-proexponential factor *a*, indicating a >7-fold increase in the enzyme activity (Table 4). With increasing chain lengths, a progressive decrease in the extent of activation was observed. Thus, while the enzyme modified by crotonaldehyde displayed a 4-fold higher activity ($a = 3.99$), the activation by *trans*-2-heptenal was only 1.4-fold. Further increase in chain length led to inactivation rather than activation of the enzyme. The values of *a* were 0.68 and 0.47 for C8 and C9 alkenals, indicating, respectively, 30 and 55% loss of enzyme activity within the 120 min observation period. A similar behavior was observed with the 4-hydroxyalkenals. The C6 alkenal in this series led to a 1.8-fold increase in the enzyme activity, whereas, the C8 to C10 alkenals lead to 40−50% loss in the enzyme activity. Interestingly, with 4-hydroxy *trans*-pentenal, the initial activation (2.4-fold) was transient, followed by a decrease in the enzyme activity to 31% of the original value. Incubation of the AR with trans,trans-2,4-alkadienals, however, had no significant effect on the enzyme activity (data not shown).

To examine the chemical mechanism by which unsaturated aldehydes modify AR, their reactivity with thiols and amines were examined. Incubation of equimolar trans-2-alkenals with GSH at room temperature and neutral pH resulted in spontaneous conjugation of alkenals with the sulfhydryl group of GSH (Table 5). The short-chain aldehydes reacted faster than the lower chain aldehydes. The rate of reaction of acrolein with GSH was more than 25-fold faster than that observed with crotonaldehyde and GSH. The rate of GSH conjugate formation decreased further with increase in the hydrocarbon chain of the alkenals. Comparing C5 to C10 alkenals, the presence of a hydroxyl group at the fourth carbon of the hydrocarbon chain increased the rate of enal:

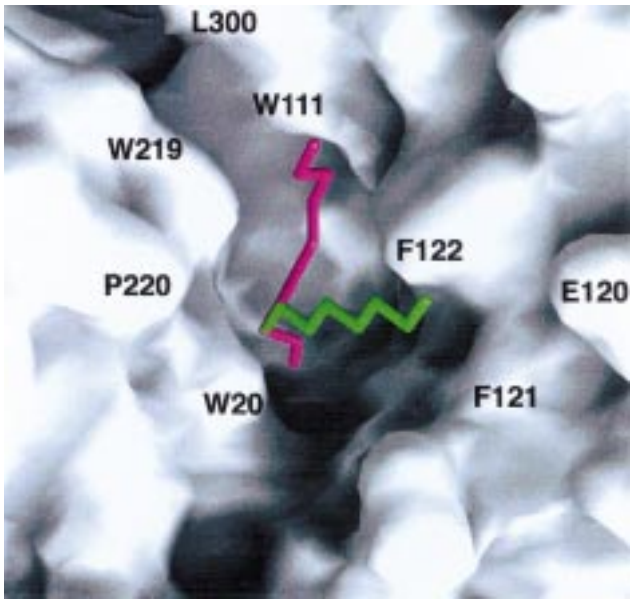

FIGURE 3: Molecular modeling of nonanal bound at the active site of aldose reductase. Two possible extended chain conformations of nonanal are shown in magenta and green. The surface of aldose reductase [generated with the program GRASP (*32*)] is colored white, red, and blue to represent regions of neutral, positive, and negative electrostatic potential, respectively. Electrostatic potentials were calculated with GRASP using an all atom charge distribution and mapped onto the molecular surface of aldose reductase.

Table 4: Rate of Modification of Aldose Reductase Activity by Unsaturated Aldehydes[a]

treatment	*a*	*b*	min
AR			
+ acrolein[b]	7.26 ± 0.03	2.34 ± 0.14	4.8 ± 0.8
+ crotonaldehyde[b]	3.99 ± 0.08	1.15 ± 0.05	8.3 ± 0.9
+ *trans*-2-pentenal[b]	2.13 ± 0.08	1.08 ± 0.09	17.9 ± 4.4
+ *trans*-2-hexenal[b]	1.77 ± 0.04	0.76 ± 0.08	6.2 ± 1.6
+ *trans*-2-heptenal[b]	1.41 ± 0.04	0.43 ± 0.05	20.8 ± 6.6
+ *trans*-2-octenal[b]	0.68 ± 0.02	0.34 ± 0.04	12.2 ± 3.5
+ *trans*-2-nonenal[b]	0.47 ± 0.04	0.56 ± 0.08	9.5 ± 3.3
+ 4-hydroxy *trans*-2-pentenal[d]	0.31 ± 0.07	2.39 ± 0.12	2.1 ± 0.2 (1) 6.64 ± 0.6 (2)
+ 4-hydroxy *trans*-2-hexenal[c]	1.79 ± 0.02	0.81 ± 0.03	10.2 ± 0.1
+ 4-hydroxy *trans*-2-octenal[c]	0.56 ± 0.05	0.46 ± 0.09	3.2 ± 1.5
+ 4-hydroxy *trans*-2-nonenal[c]	0.42 ± 0.001	0.57 ± 0.02	3.6 ± 0.3
+ 4-hydroxy *trans*-2-decenal[c]	0.54 ± 0.02	0.47 ± 0.03	2.8 ± 0.5

[a] Reduced AR (0.5 mg/mL) was treated with 100 μM alkenals at 25 °C in 0.1 M potassium phosphate, pH 7.0. Aliquots of the enzyme were withdrawn at different time intervals and the enzyme activity was measured as described in the text using DL-glyceraldehyde as the substrate for a maximal observation time of 120 min. [b] Parameters obtained from best fit of the data to the equation $y = a - b \exp(1 - t/\tau)$. [c] Parameters obtained from best fit to the equation $y = a + b \exp(-t/\tau)$. [d] Parameters obtained from the best fit to the equation $y = a - b \exp(-t/\tau_1) + c \exp(-t/\tau_2)$ for $c = 3.07$. In each case t is the time and R^2 values of the fit were between 0.996 and 0.999. Note: values of a and $b > 1$ represent activation, whereas, those < 1 represent inactivation of the enzyme.

GSH adduct formation by 4−8-fold. Introduction of an additional double bond between C_4 and C_5 of the hydrocarbon chain, however, completely abrogated their reactivity with GSH. Acrolein also reacted with lysine at neutral pH and room temperature, though the rate of reaction was much slower than acrolein:GSH conjugation. The time constant (τ) for the formation of acrolein: lysine adduct was >90-fold higher than that for the formation of the acrolein:GSH conjugate (data not shown).

Table 5: Kinetic Parameters for the Enal-GSH Conjugation[a]

	kinetic parameter		
treatment	*a*	*b*	min
GSH +			
acrolein	0.55 ± 0.01	0.73 ± 0.02	2.7 ± 0.2
crotonaldehyde	0.51 ± 0.01	0.74 ± 0.01	51.6 ± 0.5
trans-2-pentenal	0.54 ± 0.01	0.47 ± 0.01	129.4 ± 4.9
trans-2-hexenal	0.45 ± 0.02	0.53 ± 0.02	172.3 ± 14.6
trans-2-heptenal	0.39 ± 0.04	0.60 ± 0.04	184.5 ± 21.8
trans-2-octenal	0.38 ± 0.04	0.61 ± 0.04	193.3 ± 24.0
trans-2-nonenal	0.33 ± 0.05	0.64 ± 0.05	217.4 ± 29.6
4-hydroxy *trans*-2-pentenal	0.71 ± 0.01	0.26 ± 0.008	18.9 ± 1.7
4-hydroxy *trans*-2-hexenal	0.68 ± 0.005	0.36 ± 0.006	38.8 ± 1.7
4-hydroxy *trans*-2-octenal	0.65 ± 0.004	0.37 ± 0.005	40.5 ± 1.5
4-hydroxy *trans*-2-nonenal	0.76 ± 0.005	0.32 ± 0.006	35.0 ± 1.7
4-hydroxy *trans*-2-decanal	0.69 ± 0.004	0.35 ± 0.001	40.5 ± 1.5
2,4-*trans*,*trans*-hexadienal	1.02 ± 0.001		1926 ± 77
2,4-*trans*,*trans*-heptadienal	0.97 ± 0.003		1806 ± 153
2,4-*trans*,*trans*-nonadienal	0.97 ± 0.003		1832 ± 181
2,4-*trans*,*trans*-decadienal	0.96 ± 0.005		1245 ± 181

[a] The indicated aldehydes were incubated with GSH (80 μM) at 25 °C in 0.1 M potassium phosphate, pH 7.0, and the adduct formation was followed by measuring a decrese in A_{210} for acrolein, A_{224} for other alkenals and 4-hydroxyalkenals, and A_{280} for alkadienals. The time constant for the rate of loss of absorbance was calculated using the equation $y = a + b \exp(-t/\tau)$ for alkenals and 4-hydroxyalkenals, and the equation $y = a \exp(-t/\tau)$ for alkadienals. The R^2 values of the fits were 0.9998−1.0.

ESI-MS of Enal-Modified AR. As shown in Figure 4 A, the ESI-MS of the native, reduced AR (labeled "N" in the figure) displayed a major peak corresponding to a molecular mass of 35 720.8 ± 3.0 Da ($n = 7$), which is close to the expected molecular mass of 35 722.3 Da. The error in the determined molecular mass of AR was similar to that observed for the standard proteins apomyoglobin and bovine serum albumin that were used to calibrate the instrument. Significant amounts of two other species corresponding to 20 987.0 ± 1.5 ($n = 4$) Da and 14 734.1 ± 0.9 ($n = 9$) Da were also observed in the untreated enzyme sample. Examination of the amino acid sequence for the enzyme indicated a possible source for the 20 987 and 14 734 Da species as the respective Y and B fragments obtained from the cleavage of the protein at the Val 131−Pro 132 amide bond.

To examine the structural changes due to modification with acrolein, the enzyme was incubated with 100 μM acrolein for 20 min at room temperature in 0.1 M phosphate, pH 7.0. The reaction was terminated by rapid gel filtration on a nitrogen-saturated PD-10 column as described in the Materials and Methods. The ESI-MS analysis showed that the enzyme was completely modified, and the prominent species had a molecular mass of 35 778.7 Da (Figure 4 B). Upon subtracting the molecular mass of untreated AR, a measured net increase of 57.9 Da was calculated, which is consistent with the addition of a single acrolein molecule to the protein. The expected increase in the molecular mass due to the formation of such an adduct with acrolein is 56.06 Da. Furthermore, the peptide Y was not affected by acrolein, whereas the molecular mass of the peptide B was increased by 57.4 Da upon treatment with acrolein (Table 6), which suggests the formation of an adduct with C-terminal part of the protein. A deviation of 1.34−1.84 Da between the predicted and expected molecular mass is well within the error limit of these analyses. In addition to the +56 Da species, the acrolein-modified enzyme also showed another species corresponding to +87.7 Da, both in the whole protein

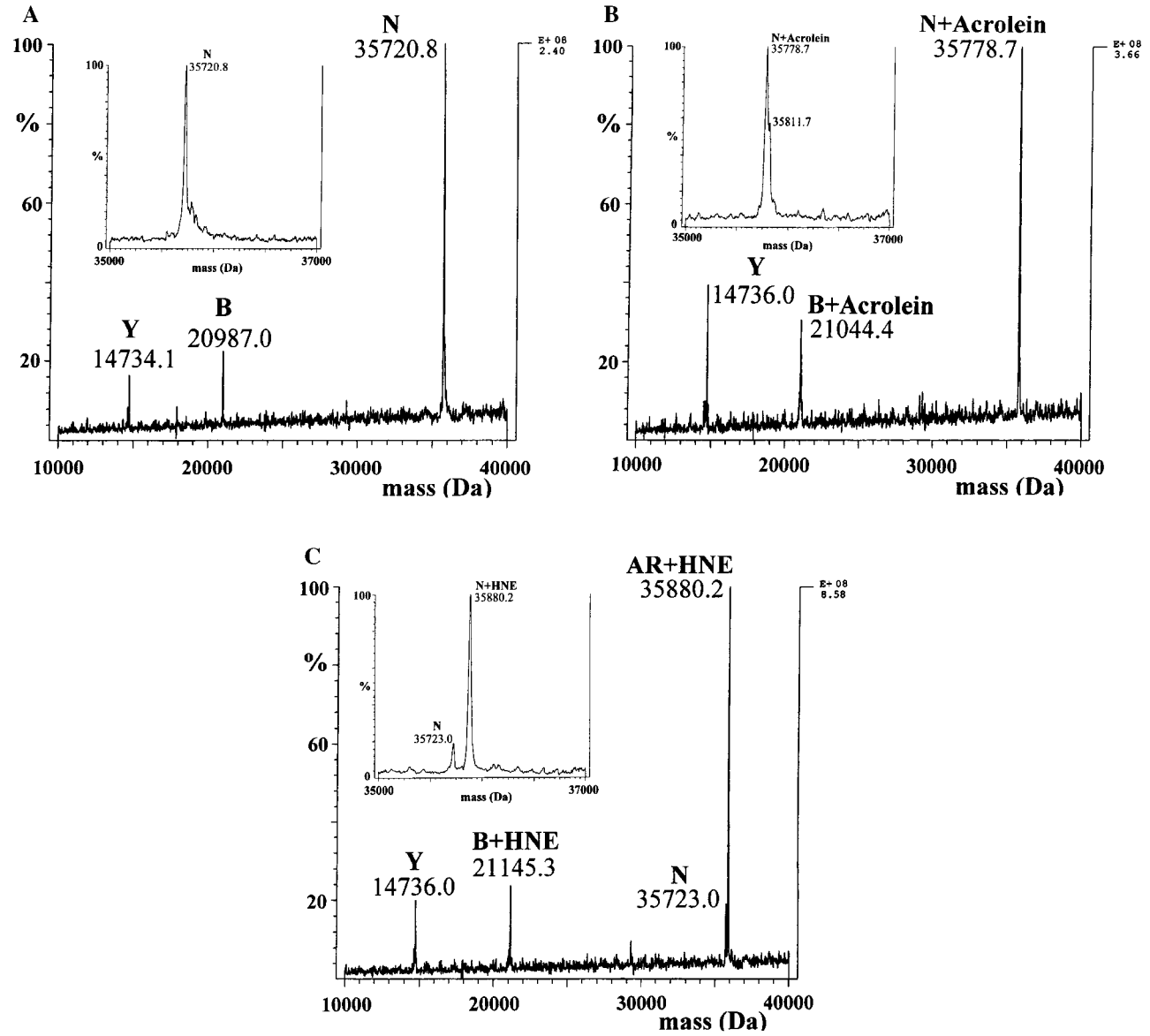

FIGURE 4: ESI-MS spectra of reduced (panel A), acrolein (panel B), and 4-hydroxy-*trans*-2 nonenal (HNE; panel C)-treated human recombinant aldose reductase (AR). The enzyme was treated with 100 μM acrolein for 20 min and 100 μM HNE for 1 h. Excess enal was removed by rapid gel filtration using N_2-saturated 10 mM ammonium acetate. Panel A shows the spectrum with a major species N, corresponding to the native enzyme (35 720.8 Da) and two minor peaks Y (14 734.1 Da) and B (20 987.0 Da) corresponding to the protein fragments from Met-1 to Val-131 and Pro-132 and Phe-312, respectively. Spectrum in the panel B shows a major species corresponding to AR covalently modified by one acrolein molecule (35 778.7 Da). Panel C show the major species corresponding to the molecular mass of AR bound to one molecule of HNE (35 880.2). The peak with a molecular mass of 35 723.1 Da in panel C corresponds to the unmodified AR. Note that the peptide fragment Y is unaffected by the treatment with acrolein, or HNE, whereas the molecular mass of fragment B in Panels B and C increased by 57.4 Da, and 158.3 Da, consistent with the addition of a single molecule of acrolein, or HNE to the C-terminal part of AR. The insets show the major peak(s) at higher resolution. The spectrum of the acrolein-treated AR shows another minor species corresponding to the molecular mass of 35 811.7 Da as a shoulder. A block temperature = 251 °C and a repeller voltage = 9 V were used for all measurements.

as well as peptide B. The nature of this species is presently unclear. However, no evidence for the formation of a Schiff base (expected molecular mass = +94 Da) was obtained from ESI-MS of acrolein-modified AR.

As shown in Table 4, modification of AR with crotonaldehyde also leads to activation of the enzyme. Crotonaldehyde-modified AR displayed two major species on ESI-MS. The predominant species had a molecular mass of 35 792.7 Da (molecular mass of native AR + 69.7), which is consistent with the formation of a 1:1 protein:crotonaldehyde adduct (expected increase in molecular mass = 70.09). The second species of the crotonaldehyde-modified AR corresponded to a molecular mass of 35 823.8 Da, which is +100.8 Da more than untreated AR (or 31.1 Da more than crotonaldehyde-AR adduct). Similar to acrolein modification, the peptide Y was not affected by crotonaldehyde, whereas peptide B showed both the +70 and +100.8 species observed with the whole protein. The remaining 30% of AR showed a molecular mass of 35 723.1, which corresponds to that of the native enzyme (Table 6).

In contrast to crotonaldehyde and acrolein, exposure to HNE led to inactivation of AR (Table 4). The HNE-modified enzyme displayed two major species on ESI-MS corresponding to molecular mass of 35 723.0 and 35 880.2 Da (Figure

Table 6: Summary of ESI-MS Measurements of Wild-Type and Site-Directed Mutant Forms of AR Treated with 4-Hydroxy-*trans*-2-nonenal and Acrolein[a]

	peaks									
	Y		*B*				*N*			
	expected	measured	expected	measured	measured mass		expected	measured	measured mass	
treatment	mass	mass	mass	mass	B_1	B_2	mass	mass	M_1	M_2
AR	14 735.0	14 734.1	20 988.0	20 987.0			35 722.3	35 720.8		
+acrolein	14 735.0	14 736.0	20 988.0	ND	21 044.4	21 074.2	35 722.3	ND	35 778.4	35 811.7
+crotonal	14 735.0	14 737.5	20 988.0	20 988.2	21 058.6	21 089.7	35 722.3	35 723.1	35 792.7	35 823.8
+ HNE	14 735.0	14 736.0	20 988.0	20 988.1	21 145.3		35 722.3	35 723.0	35 880.2	
AR:C303 + acrolein	14 735.0	ND		ND	2104.4	21 075.6		ND	35 761.8	35 792.8
AR:C298	14 735.0	ND	20 972.0	ND			35 706.3	35 705.8		
+ acrolein	14 735.0	14 736.0	20 972.0	20 973.1			35 706.3	35 710.1		

[a] The enzymes were treated with the indicated aldehyde as described in the text. The molecular mass of acrolein, crotonaldehyde and HNE is 56.1, 70.1, and 156 Da, respectively. ND, not detected. Peak *N* refers to the covalent modification of AR by the indicated aldehyde. Peak *Y* is due to AR fragment from Met-1 to Val-131, and peak *B* is due to AR fragment from Pro-132 to Phe-312. Peaks B_1 and B_2 are due to covalent modification of AR fragment by the indicated aldehyde. M_1 and M_2 are the modified protein peaks.

4C). The first species represents unreacted AR, whereas the second species (AR + 157.2 Da) is consistent with the formation of an 1:1 adduct between AR and HNE. Similar to acrolein and crotonaldehyde, the peptide Y did not react with HNE whereas the molecular mass of peptide B increased by 157.6 Da, suggesting adduct formation with the C-terminal of AR (Table 6).

To identify the site of modification of AR by enals, mutant forms of AR were used, in which the solvent exposed cysteines located at positions 298 and 303 were individually replaced by serine. These site-directed mutant forms of AR were reduced exhaustively and incubated with acrolein under conditions identical to those used to modify the wild-type AR. The ESI-MS of untreated AR:C298S corresponded to a molecular mass of 35 705.8 Da, which is in agreement with the sequence-predicted molecular mass of 35 706.3 Da for this form of AR (Table 6). The acrolein-treated AR:C298S also resolved as a single peak corresponding to a molecular mass of 35 710.1 Da demonstrating no significant changes in the molecular mass upon incubation with acrolein. In parallel kinetic experiments, incubation of AR:C298S with either acrolein or HNE led to no significant change in the enzyme activity, indicating that AR:C298S is insensitive to enal modification. In contrast, acrolein-treated AR:C303S showed the formation of +56 and +86 Da species, both in the whole protein as well as the peptide B, a pattern identical to that observed with the wild-type enzyme (Table 6).

DISCUSSION

Despite the well-documented injurious effects of AR under hyperglycemia (*1*, *2*), the normal physiological role of the enzyme remains obscure. An understanding of the normal metabolic function(s) of AR is particularly important since AR is a potential target for the treatment of long-term diabetic complications. The proposed therapy with AR inhibitors is likely to be long-term and leads to chronic inhibition of the enzyme even in tissues not exposed to hyperglycemia. Thus, elucidation of the physiological role of AR and a better understanding of its structure and function are essential for designing efficient anti-AR interventions and for assessing their long-term risks.

While the structure of AR and its mutant forms has been studied in detail, little is known in regard to its substrate-binding properties and the structural and kinetic constraints that determine its substrate specificity and catalytic efficiency. In the present study, we measured the steady-state kinetic parameters of AR with several classes of aldehydes that are generated in vivo during lipid peroxidation. The progress curve analysis with HNE suggests that, despite high reactivity of unsaturated aldehydes with the free enzyme, the steady-state kinetic parameters of these substrates are not contaminated by noncatalytic, covalent modification of the enzyme. Although, steady-state kinetic parameters usually do not correspond to unitary rate constants, in case of AR, the parameters K_m and k_{cat}/K_m approximate specific steps in the catalytic cycle. Previous studies show that AR follows a compulsory ordered bi−bi reaction scheme, in which the catalytic rate is limited by release of NADP (*33*, *34*). In this reaction sequence (Scheme 1),

Scheme 1

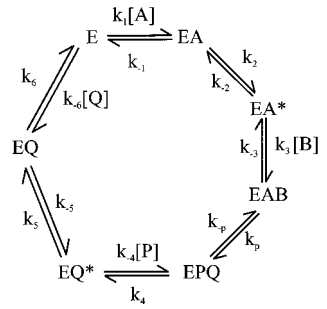

$$K_B = k_2k_5k_6(k_{-3}k_{-p} + k_{-3}k_4 + k_pk_4)(1 + k_{-2}/k_2)/[k_2k_3k_pk_4 (k_5 + k_{-5} + k_6) + k_2k_3k_5k_6(k_6 + k_{-p} + k_4) + k_3k_pk_4k_5k_6] \quad (1)$$

$$k_{cat}/K_B = k_3k_pk_4/[k_{-3}k_{-p} + k_{-3}k_4 + k_pk_4)(1 + k_{-2}/k_2) \quad (2)$$

Since for AR, $k_{-p} \ll k_4$ and $k_{-2} \ll k_2$ (*35*),

$$k_{cat}/K_B = k_3k_p/(k_{-3} + k_p) \text{ or } k_3/(1 + k_{-3}/k_p) \quad (3)$$

$k_{-3}/k_p \approx 0.2$ so that $V/K_B \approx k_3$ and $V/[E]_t = k_{cat} = k_5$ and $K_B = V_f/(V_f/K_B) = k_5/k_3$ (4)

therefore, the K_m of the enzyme for the aldehyde substrate

is equal to the forward isomerization rate constant (k_5) divided by the rate constant for the substrate binding (k_3); and for similar k_5 values, k_{cat}/K_m corresponds approximately to the unitary on-rate constant of aldehyde binding to the enzyme (k_3).

For a homologous series of substrate, the incremental Gibbs free-energy change associated with the rate constant k_{cat}/K_m could be calculated relative to the lowest member of the series (propanal):

$$\Delta\Delta G_b = -RT \ln[k_{cat}/K_{m(CH_3-(CH_2)_x-CHO}/(k_{cat}/K_m)_{(CH_3-CH_2-CHO)}] \quad (5)$$

where x is the number of methylene groups of R. From this relationship, the total maximal binding energy contributed by the hydrophobic interaction with alkanals is about 2−4 kcal/mol. A progressive increase in $\Delta\Delta G_b$ was observed going from C4 to C6 alkanal, indicating additional interactions with an increased length of the methylene side chain. The $\Delta\Delta G_b$, however, decreased for alkenals greater than C6 presumably due to the entropic cost of constraining long methylene chains. A plot of $-\Delta\Delta G_b$ versus incremental Gibbs free energy of transfer of the group R from *n*-octanol to water ($=2.303RT\pi$; where π is the hydrophobicity coefficient of R relative to the hydrogen atom) was linear for C2 to C5 alkanals, with a slope of 2.5 (data not shown), indicating that the active site of human AR is 2.5 times more hydrophobic than *n*-octanol, and 1.7 times more hydrophobic than the active site of the yeast AR (*36*). The high hydrophobicity of the active site suggests efficient interaction of the active site with long-chain aldehydes.

While previous studies have suggested hydrophobic interactions in substrate binding, the role of these interactions could not be clearly delineated, since polyhydroxylated aldehydes were used (*37*). With these compounds, potential binding via hydrogen bonds could obscure clear delineation of the hydrophobic interactions. In the present study, straight-chain alkanals and alkenals were used, which cannot form hydrogen bonds with the active-site residues. Nevertheless, a striking increase in catalytic efficiency was observed upon increasing the methylene chain length of all the classes of aldehydes tested, clearly indicating the importance of hydrophobic interactions. Quantitatively, a maximal free energy change of 3−4 kcal/mol could be achieved by hydrophobic interactions alone (comparing propanal and hexanal). Since these values correspond to the free-energy change due to the formation of a hydrogen bond, it appears that AR is capable of using hydrophobic interactions to achieve substrate specificity of the order of that provided by interactions via hydrogen bonds.

Due to the presence of an OH group at C_4, HNE, and related 4-hydroxyalkenals could potentially participate in hydrogen bond formation. However, our modeling studies suggest little or no interaction between the 4-OH of 4-hydroxyalkenals with the enzyme residues. This was somewhat surprising, since on the basis of the high affinity of the enzyme for HNE (*9, 10*), we expected specific interaction between the enzyme and 4-hydroxyalkenals. Nonetheless, the absence of hydrogen bonds suggests that the high efficiency of AR with HNE is also due to increased hydrophobic interactions. Substrate recognition via hydrophobic interactions rather than hydrogen bonds may serve to extend the range of aldehydes which could be reduced by the enzyme. Apparently, due to this mode of selection, the enzyme is capable of efficiently reducing alkanals and alkenals of diverse structure. These aldehydes can be accommodated at the active site, without a change in its structure or the movement of side chains. The lack of large conformational changes for aldehyde binding will further minimize the energetic cost of substrate binding and afford a wider substrate selection.

Hydrophobic interactions, however, do not appear to be the sole determinant of aldehyde selectivity. A comparison of the catalytic efficiencies of alkanals, alkenals, and alkadienals shows in general a progressive decrease with an increase in the number of double bonds in the substrate (=0, 1, and 2, respectively). The addition of double bond provides greater rigidity to the molecule, which may sterically limit the optimal orientation of the substrate in the AR-binding site. Since the enzyme displays high efficiency with hexanal, it appears that for small methylene chain aldehydes (< C7), interaction in the nonextended form is preferred (the corresponding alkenals and alkadienals show much lower values of k_{cat}/K_m). However, for long-chain aldehydes (>C8), the situation is reversed and the extended form appears to be preferred (the alkenals have much higher k_{cat}/K_m values than the corresponding alkanals). Nevertheless, even with long methylene chains, the alkadienal conformation appears not be preferred. As a result of this switching of the binding mode, hexanal and *trans*-2-nonenal are the best substrates in their respective series.

In addition to aldehyde conformation, changes in the structure of the side chain (branched or unbranched) also caused profound alterations in catalytic efficiency of the enzyme. This is most clearly seen with acrolein and its derivatives. While unsubstituted acrolein was a poor substrate, addition of longer side chains (ethyl, butyl, phenyl, and methyl phenyl) led to a progressive increase in k_{cat}/K_m. More extensive energy stabilization was observed with methyl phenyl acrolein, which displayed an approximately 2 kcal/mol greater binding energy as compared to acrolein. Since the binding of zopolrestat is stabilized due to stacking of its aromatic groups against the aromatic residues at the active site (*30*), it appears likely that similar interactions may also account for the high catalytic efficiency displayed by aromatic substituents of acrolein. Moreover, even though increasing hydrophobicity due to an increasing linear methylene chain of the alkanals from C6 to C10 does not translate into enhanced catalytic efficiency, branched chain substrates displayed better catalytic efficiency (compare ethyl acrolein with *trans*-2-pentenal and 2-butyl acrolein with *trans*-2-hexenal; Tables 1 and 2). These results suggest that branched- or parallel-chain substrates that "fill up" the active site are likely to be the preferred substrates. This view is further supported by the observation that the highest free-energy change was associated with the glutathione conjugate of acrolein (GS-propanal). The GS-propanal displayed approximately 4 kcal/mol greater free-energy changes and 2 orders of magnitude greater k_{cat}/K_m values as compared to propanal. Indeed, of all the substrates tested, the enzyme showed the highest k_{cat}/K_m and the lowest K_m values for GS-propanal. In conjunction with our previous observations that the enzyme displays high activity with GS-4-hydroxynonanal (*10*), and that in perfused hearts AR inhibitors prevent the

reduction of GS-4-hydroxynonanal to GS-1,4-dihydroxynonanol (*38*), it appears that reduction of glutathione conjugates may be one of the physiological function of AR.

That the active site can efficiently bind two parallel-chain substrates is also suggested by our active-site modification studies. Incubation of the enzyme with acrolein led to a 7-fold increase in the catalytic activity of the enzyme (measured with DL-glyceraldehyde). Several lines of evidence suggest that this activation is due to modification of the active-site cysteine (Cys 298), and not to a lysine residue (cf. *39*). These include (a) the high intrinsic reactivity of alkenals with thiols (GSH) as compared to amines, (b) the ESI-MS results which show a single molecule of acrolein is bound to the enzyme, and (c) the insensitivity of the AR mutant C298S to acrolein and its lack of modification upon incubation with acrolein. On the basis of these observations and previous results obtained from the analysis of HNE-modified AR (*4*, *40*), we conclude that both activation (by acrolein and crotonaldehyde) as well as inactivation (by HNE) are due to modification of Cys 298 present at the active site. While the elucidation of the structural changes leading to activation or inactivation must await X-ray analysis of the crystals of the modified enzyme, it appears reasonable to suggest that the inactivation by long methylene chain alkenals (as opposed to activation by short-chain alkenals) may be due to occlusion of the active site by long methylene chains. However, the marked activation of the enzyme with acrolein clearly indicates that in addition to the aldehyde molecule bound to the catalytic center, the enzyme is capable of binding another molecule of the substrate to another domain of the active site. Simultaneous binding of two aldehydes to the active site is likely to be analogous to the "double decker" binding of two inhibitor molecules to the active site of the enzyme (*41*). Thus, for highest catalytic efficiency, binding of parallel or branched substrates leading to a distention of the active site may be necessary.

On the basis of the kinetic and thermodynamic properties of the enzyme, it has been suggested that AR represents a novel paradigm of enzyme perfection (*37*). Since the enzyme binds NADPH very tightly and the turnover rate of the enzyme is limited by the release of NADP, it was pointed out that the energy for stabilization of the transition state may be entirely derived from the interaction of the enzyme with NADPH and that no additional energy is realized from the interaction between the aldehyde and the E:NADPH binary complex. It was suggested that the formation of E:NADPH results in the generation of a "super-reactive" enzyme that catalyzes an essentially "one-way" reduction of a wide range of substrates (*37*). This view is supported by the observations that (a) the k_{cat} of AR does not vary over a wide range of substrate (aldehyde) structure and (b) the catalytic efficiencies of the enzyme for the reduction of various poly-hydroxylated substrates are fairly constant once correction is made for the free aldehyde present in solution. Our present results, however, do not support the view of aldose reductase as a nonspecific aldehyde reductase. In agreement with the previous reports (*37*, *42*), we observed no large changes in the k_{cat} of the enzyme over a wide range of aldehyde structures, even though the K_m values varied over several orders of magnitude. It should, however, be pointed out that the k_{cat} values did show small, but significant differences (2−3-fold) over the range of aldehydes studied, indicating a small contribution of aldehyde binding to the overall rate. Regardless, we interpret the insensitivity of the k_{cat} values to the aldehyde structure as a reflection of the slow isomerization rate of the E:NADP complex. Whether the insensitivity of k_{cat} indicates that the aldehyde substrate does not contribute to the stabilization of the transition state is not clear. On the contrary, we observed 10^2-10^3-fold differences in the catalytic efficiency of the enzyme with various aldehydes tested. Since this corresponds to a free-energy change of 2−4 kcal/mol, it appears unlikely that the ground-state interaction between the aldehyde and E:NADPH is energetically inconsequential and does not affect the stabilization of the transition state. On the basis of our current data, we suggest instead that the wide substrate specificity of AR is due to its ability to bind aldehydes efficiently via hydrophobic interactions (as opposed to hydrogen bonds). The energy cost of aldehyde binding is minimized by the large and hydrophobic active site that does not necessitate large conformational changes or extensive movement of side chains (vide supra).

Finally, our in vitro data suggest novel in vivo role(s) of AR. In each of the series of the aldehydes tested, AR was found to display highest catalytic efficiency with the aldehydes expected to be generated in highest concentrations during in vivo lipid peroxidation, i.e., hexanal, *trans*-2-nonenal, HNE, and *trans*,*trans*-2,4-nonadienal. During autoxidation, hexanal is the major product generated from linoleic and arachidonic acids, accounting for 66.4 and 31.8% of the volatile carbonyl compounds; other aldehydes such as octenal, *trans*-2-*cis*-4-decadienal, and *trans*-2-heptenal constitute 10−15% of the carbonyls (*19*). Peroxidation of cardiac, renal, and hepatic tissues (*43*, *44*) of course generates high concentrations of HNE [which in some cases accounts for 95% of the unsaturated aldehydes formed (*45*)], although elevated concentrations of the saturated aldehydes, pentanal and hexanal, as well as unsaturated aldehydes such as *trans*,*trans*-2,4-nonadienal, *trans*-2-nonenal, and *trans*-2-octenal also are observed. Little or no formation and accumulation of short-chain alkenals has been observed both in vivo and in vitro. Thus, AR displays selectively high catalytic efficiency with precisely the same aldehydes which represent the major endproducts of lipid peroxidation. Furthermore, the K_m of AR for these aldehdyes is well within their expected physiological and pathological concentrations. It has been estimated that, during microsomal peroxidation, the effective concentration of unsaturated aldehydes may be between 10 and 100 mM (*46*, *47*), and although these aldehydes are rapidly metabolized, their steady-state concentrations during several pathological states can be between 1 and 40 μM (*11*).

While short-chain aldehydes are generally minor products of autoxidation of polyunstaturated fatty acids, acrolein may be an exception. Acrolein has recently been identified as a significant product of LDL oxidation (*20*). In addition, myeloperoxidase-catalyzed oxidation of amino acids (*48*), as well as the oxidation of polyamines (*49*) leads to the generation of high concentrations of acrolein. Thus, our observation that AR catalyzes the reduction of acrolein and its mercapturic acid and glutathione derivatives (the principal in vivo metabolites of acrolein) suggests that the endogenous levels of AR may be an important determinant of tissue injury due to chronic inflammation. In addition, AR-catalyzed

pathways may also be important in environmental and drug toxicities. Unsaturated aldehydes are ubiquitous constituents of pollutants [high concentrations of acrolein are generated during incomplete combustion of fossil fuels, plastics and polyethylene and tobacco smoke (*50*)] or are generated during the metabolism of several foods such as senecione alkaloids which generate 4-hydroxyhexenal (*51*), toxicants such as nitropropanol (*52*) and allylamine (*53*), butadiene (*54*) and drugs such as cyclophoshamide (*55*) and felbamate (*56*).

Catalysis of alkanal reduction by AR may also be an important metabolic function of AR. Due to the absence of a conjugated system, these aldehydes do not readily form conjugates with GSH, but are metabolized as such to acyloins and alcohols. The latter, as suggested by the present study, is generated possibly by AR-mediated catalysis. While less cytotoxic than alkenals, saturated aldehydes are more potent inhibitors of cytochrome P450 than alkenals and 4-hydroxyalkenals (*57*). Similarly, although the conjugation of alkenals with GSH (which converts alkenals to alkanals) is generally considered to be a detoxification process, in several instances, the glutathione conjugation leads to metabolic "activation" of toxic aldehydes. The GS-propanal, for example, is markedly nephrotoxic (*58*), and a more potent stimulator of oxygen radical formation than acrolein (*59*), and the GS-conjugates of hexenal and nonadienal induce DNA damage (*60*). In addition, the GS-aldehyde adducts inhibit glutathione S-transferases (*61*). Thus, in addition to a direct metabolism, AR may secondarily provide protection against aldehyde toxicity by preventing the inactivation of the other detoxification enzymes. Such protective functions of AR would place it well within the detoxification triad consisting of glutathione S-transferases and cytochrome P450s. Thus, taken together, our results suggest that in addition to osmoregulation and sorbitol formation, AR catalysis may be an important determinant of tissue injury during several pathological and toxicological states, associated with excessive aldehyde generation.

REFERENCES

1. Bhatnagar, A., and Srivastava S. K (1992) *Biochem. Med. Metab. Biol. 48*, 91−121.
2. Kinoshita, J. H., and Nishimura, C. (1988) *Diabetes Metab. Rev. 4*, 323−337.
3. Cao, D., Tat Fan, S., and Chung, S. S. M. (1998) *J. Biol. Chem. 273*, 11429−11435.
4. Srivastava, S., Chandra, A., Ansari, N. H., Srivastava, S. K., and Bhatnagar, A. (1998) *Biochem. J. 329*, 469−475.
5. Van der Jagt, D. L., Robinson, B., Taylor, K. K., and Hunsaker, L. A. (1990) *J. Biol. Chem. 265*, 20982−20987.
6. Van der Jagt, D. L., Robinson, B., Taylor, K. K., and Hunsaker, L. A. (1992) *J. Biol. Chem. 267*, 4364−4369.
7. Wilson, D. K., Bohren, K. M., Gabbay, K. H., and Quiocho, F. A. (1992) *Science 257*, 81−84.
8. Flynn, T. G. (1982) *Biochem. Pharmacol. 31*, 2705−2712.
9. Vander Jagt, D. L., Kolb, N. S., Vander Jagt, T. J., Chino, J., Martinez, F. J., Hunsaker, L. A., and Royer, R. E. (1995) *Biochim. Biophys. Acta 1249*, 117−126.
10. Srivastava, S., Chandra, A., Bhatnagar, A., Srivastava, S. K., and Ansari, N. H. (1995) *Biochem. Biophys. Res. Commun. 217*, 741−746.
11. Esterbauer, H., Schaur, R. J., and Zollner, H. (1991) *Free Rad. Biol. Med. 11*, 81−128.
12. Yla-Herttuala, S., Palinski, W., Rosenfeld, M. E., Parthasarathy, Carew, T. E., Butler, S., Witztum, J. L., and Steinberg, D. (1989) *J. Clin. Invest. 84*, 1086−1095.
13. Sayre, L. M., Zelasko, D. A., Harris, P. L., Perry, G., Salomon, R. G., and Smith, M. A. (1997) *J. Neurochem. 68*, 2092−2097.
14. Yoritaka, A., Hattori, N., Uchida, K., Tanaka, M., Stadtman, E. R., and Mizuno, Y. (1996) *Proc. Natl. Acad. Sci. U.S.A. 93*, 2696−2701.
15. Chen, P., Wiesler, D., Chmelik, J., and Novotny, M. (1996) *Chem. Res. Tox. 9*, 970−979.
16. McCall, M. R., Tang, J. Y., Bielicki, J. K., Forte, T. M. (1995) *Arterioscler. Thromb. Vasc. Biol. 15*, 1599−1606.
17. Ruef, J., Rao, G. N., Li, F, Bode, C., Patterson, C., Bhatnagar, A., and Runge, M. S. (1998) *Circulation 97*, 1071−1078.
18. Butterfield, D. A. (1997) *Chem. Res. Toxicol. 10*, 495−506.
19. Grosch W. in *Autoxidation of Unsaturated Lipids* (Chan, H. W.-S., Ed.) Academic Press, London, 1987; pp 95−135.
20. Uchida K., Kanematsu, M, Morimitsu, Y., Osawa, T., Noguchi, N., Niki, E. (1998) *J. Biol. Chem. 273*, 16058−16066.
21. Palinski, W., Horkko S., Miller E., Steinbrecher U. P., Powell, H. C., Curtiss, L. K., and Witztum, J. L. (1996) *J. Clin. Invest. 98*, 800−814.
22. Chandra, A., and Srivastava, S. K. (1997) *Lipids 32*, 779−782.
23. Marnett, L. J., and Tuttle, M. A. (1980) *Cancer Res. 40*, 276−282.
24. Petrash, J. M., Harter, T. M., Devine, C. S., Olins, P. O., Bhatnagar, A., Liu, S.-Q., and Srivastava, S. K. (1992) *J. Biol. Chem. 267*, 24833−24840.
25. Jones, T. A., Zou, J.-Y., Cowan S. W., and Kjeldgaard, M. (1991) *Acta Crystallogr.*, Sect. *A 47*, 110−119.
26. Rubenstein, S. (1993) *CSC Chem Draw Plus*, Version 3.1.
27. Cleland WW (1979) *Methods Enzymol. 63*, 103−138.
28. Duggleby, R. G. (1995) *Methods Enzymol. 249*, 61−90.
29. Harrison, D. H., Bohren, K. M., Ringe, D., Petsko, G. A., and Gabbay, K. H. (1994) *Biochemistry 33*, 2011−2020.
30. Wilson, D. K., Tarle, I., Petrash, J. M., Quiocho, F. A. (1993) *Proc. Natl. Acad. Sci. U.S.A. 90*, 9847−9851.
31. DeWinter, H. L., and von Itzein, M. (1995) *Biochemistry 34*, 8299−8308.
32. Nichols, A., Sharp K. A., and Honig, B. (1991) *Proteins 11*, 281−296.
33. Grimshaw C. E., Shahbaz, M., and Putney, C. G. (1990) *Biochemistry 29*, 9947−9955.
34. Kubiseski, T. J. Hyndman D. J., Morjana, N. A., and Flynn, T. G. (1992) *J. Biol. Chem. 267*, 6510−6517.
35. Grimshaw, C. E., Bohren, K. M., Lai, C.-J., and Gabbay, K. H. (1995) *Biochemistry 34*, 14366−14373.
36. Neuhauser, W., Haltrich, D., Kulbe, K. D., Nidetsky, B. (1998) *Biochemistry 37*, 1116−1123.
37. Grimshaw C. E. (1992) *Biochemistry 31*, 10139−10145.
38. Srivastava S. Chandra A, Wang, L.-F., Seifert, W. E., DaGue, B. B., Ansari, N. H., Srivastava, S. K., and Bhatnagar, A. (1998) *J. Biol. Chem. 273*, 10893−10900.
39. Kolb, N. S., Hunsaker, L. A., and Van der Jagt, D. L. (1994) *Mol. Pharmacol. 45*, 797−801.
40. Del Corso, A., Dal Monte, M., Vilardo, P. G., Cecconi, I., Moshini, R., Banditelli, S., Cappiello, M., Tsai, L., and Mura, U. (1998) *Arch. Biochem. Biophys. 350*, 245−248.
41. Harrison, D. H., Bohren, K. M., Petsko, G. A., Ringe, D., and Gabbay, K. H. (1997) *Biochemistry 36*, 16134−16140.
42. Vander Jagt, D. L., Kolb, N. S., Vander Jagt, T. J., Chino, J., Martinez, F. J., Hunsaker, L. A., and Royer, R. E. (1995) *Biochim. Biophys. Acta 1249*, 117−126.
43. Luo, X., Evrovsky, Y., Cole, D., Trines, J., Benson, L. N., and Lehotay, D. C. (1997) *Biochim. Biophys. Acta 1360*, 45−62.
44. Tokokuni, S., Luo, X.-P., Tanaka, K., Hiai, H., and Lehotay, D. C. (1997) *Free Radical Biol. Med. 22*, 1019−1027.
45. Benedetti, A., Comporti, M., and Esterbauer, H. (1980) *Biochim. Biophys. Acta 620*, 281−286.
46. Benedetti, A., Fulceri, R., Ferrali, M., Ciccoli, Esterbauer, H., and Comporti, M. (1982) *Biochim. Biophys. Acta 712*, 628−638.
47. Benedetti, A., Comporti, M., Fulceri, R., and Esterbauer, H. (1984) *Biochim. Biophys. Acta 792*, 172−181.

48. Anderson, M. M., Hazen, S. L., Hsu, F. F., and Heinecke, J. W. (1997) *J. Clin. Invest. 99*, 424−432.
49. Alarcon, R. A. (1970) *Arch. Biochem. Biophys. 137*, 365−372.
50. Ghilarducci, D. P., and Tjeerdema, R. S. (1995) *Rev. Environ. Contam. Toxicol. 144*, 95−147.
51. Segall, H. J., Wislon, D. W., Dallas, J. L., and Haddon, W. F. (1985) *Science 229*, 472−475.
52. Alson, T. A., Seitz, S. P., and Bright, H. G. (1981) *Biochem. Pharmacol. 23*, 2328−2331.
53. Boor, P. J., and Hysmith, R. M. (1987) *Toxicology 44*, 129−145.
54. Nauhaus, S. K., Fenell, T. R., Asgharian, B., and Bond, J. A. (1996) *Chem. Res. Toxicol. 9*, 764−773.
55. Anderson, D., Bishops, J. B., Garner, R. C., Ostrosky-Wegman, P., and Selby, P. B. (1995) *Mutat. Res. 330*, 115−181.
56. Thompson, C. D., Gulden, P. H., and Macdonald, T. L. (1997) *Chem. Res. Toxicol. 10*, 457−462.
57. Raner, G. M., Chiang, E. W., Vaz, A. F. D., and Coon, M. J. (1997) *Biochemistry 36*, 4895−4902.
58. Horvath, J. J., Witmer, C. M., and Witz, G. (1992) *Toxicol. Appl. Pharmacol. 117*, 200−207.
59. Adams, J. D., and Klaidman, L. K. (1993) *Free Radic. Biol. Med. 15*, 187−193.
60. Eisenbrand, G., Schumacher, J., and Golzer, P. (1995) *Chem. Res. Toxicol. 8*, 40−46.
61. Danielson, U. H., Esterbauer, H., and Mannervik, B. (1987) *Biochem. J. 247*, 707−713.

BI981794L